Alternating Oligo[(2,3-*O*-isopropylidene-L-threitol)]-*co*-[(*E*,*E*)-1,4-bis(styryl)benzene]s: The Linear Chirality Transmisson Additivity Relationship in Nematic Liquid Crystals

Li-Chung Kuo,[†] Wan-Ting Huang,[†] Kuei-Hui Yang,[†] Hsiu-Fu Hsu,[‡] Bih-Yaw Jin,[†] and Man-kit Leung*,[†]

Department of Chemistry, National Taiwan University, Taipei, Taiwan 106, Republic of China, and Department of Chemistry, Tamkang University, Taipei, Taiwan 251, Republic of China

Received: September 28, 2009; Revised Manuscript Received: January 4, 2010

Alternating oligo[2,3-*O*-isopropylidene-L-threitol]-*co*-[(*E*,*E*)-1,4-bis(styryl)benzene]s (denoted as **2**−**6** in the article) show helical twisting power (HTP), in 4-pentoxyl-4′-biphenylcarbonitrile (5OCB), linearly proportional to the number of the chiral cores in the oligomers. The HTP per chiral core of $-1.75\ \mu m^{-1}$ was recorded in the correlation plot with a correlation coefficient of $R = 0.99$. These results suggested that the C_2 chiral L-threitol cores are aligned along the same axis. The comparable linear dichroism (LD) of 0.42 ± 0.02 obtained for (*rac*)-**2**−**5** at 405 nm, and of 0.52 ± 0.03 for E7, a commercially available room temperature nematic solvent, at 347 nm in a parallel rubbed cell indicated that the long axis of the bis(styryl)benzene segments is more or less parallel to the director of the E7 in the LC matrix. This observation is highly exciting because the HTP per core could still be maintained, no matter whether the cores are evenly spread in a form of monomer in the LC matrix or tightly confined in a polymer. Theoretical treatments about the conformations of the dopant in the nematic matrix are discussed.

Introduction

Chiral-dopant-induced cholesteric liquid crystal (LC) mesophases are of particular important due to their technological applications[1] as well as fundamental interest of stereochemistry and chirality.[1,2] When chiral dopant molecules are introduced into a nematic matrix, the orientation of the nematic layers would helically rotate to form a chiral cholesteric phase (Figure 1).[3] The information on the chiral molecules are therefore expressed in the form of a long-range orientation or positional order of the LC molecules that could be observed through amplification of the quantities of the optical rotation or the circular dichroism. The cholesteric phase has a periodical helicity, in which the orientation of the long molecular axes in each successive layer forms a given angle with that of molecules in the preceding layer. Corresponding to the pitch p, the axis of orientation of the molecules, known as the director, rotates through an angle of 2π. The periodic structures were characterized by selective reflection as well as angular dependence of the reflected wavelength.[1a] The chiral-dopant effects were found even in very dilute conditions, in which one dopant molecule would influence hundreds of LC molecules.[3] Although detection of a chiral compound by its chiral induction of a cholesteric phase is a very sensitive method,[4] only for a few classes of organic dopants a qualitative correlation between the molecular structure and the induced helicity has been developed.[5−12] In order to design and develop materials with definite helical twisting power, understanding of the factors that govern the interactions between chiral dopants and nematic hosts is of special importance. During the past few decades, four major classes of chiral dopants have been designed: (1) chiral dopants without mesogenic group;[3,6] (2) chiral dopants with mesogenic group tethered with a flexible spacer;[6] (3) chiral dopants with the chiral core hooked in between two or more mesogenic groups by flexible spacers;[7,8] and (4) chiral dopants with chiral core integrated as part of the mesogenic group.[9−12] Although the chiral cores are the origin of the chiral induction, the roles of the achiral parts of the molecules are also responsible for the chirality measurements.

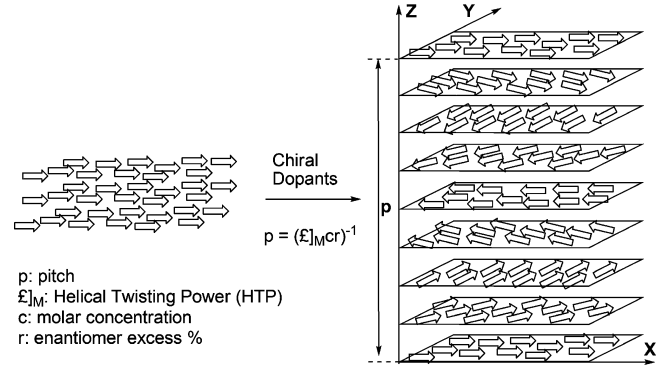

Figure 1. Chiral-dopant-induced helical twist in a nematic solvent.

TABLE 1: Calculated HTP of Dopants at 50 °C

	β_M (μm^{-1})[a]	no. of chiral cores	β_M/core
2	−3.9	2	−1.95
3	−5.2	3	−1.73
4	−7.1	4	−1.77
5	−17.6	∼10[b]	−1.76
6	−26.3	∼15[b]	−1.75
7	−6.1	1	−6.1
8	−3.8	1	−3.8
9	−3.1	1	−3.55

[a] Uncertainty on tan θ of the wedge cell: ±5%. [b] Determined by ^{1}H NMR.

The measure of the ability of a chiral molecule to produce twisted phase is called the helical twisting power (HTP, defined

* To whom correspondence should be addressed. E-mail: mkleung@ntu.edu.tw.
[†] National Taiwan University.
[‡] Tamkang University.

10.1021/jp909286t
Published on Web 02/08/2010

SCHEME 1: Structures of the L-Threitol Based Chiral Dopants and Their Synthetic Precursors

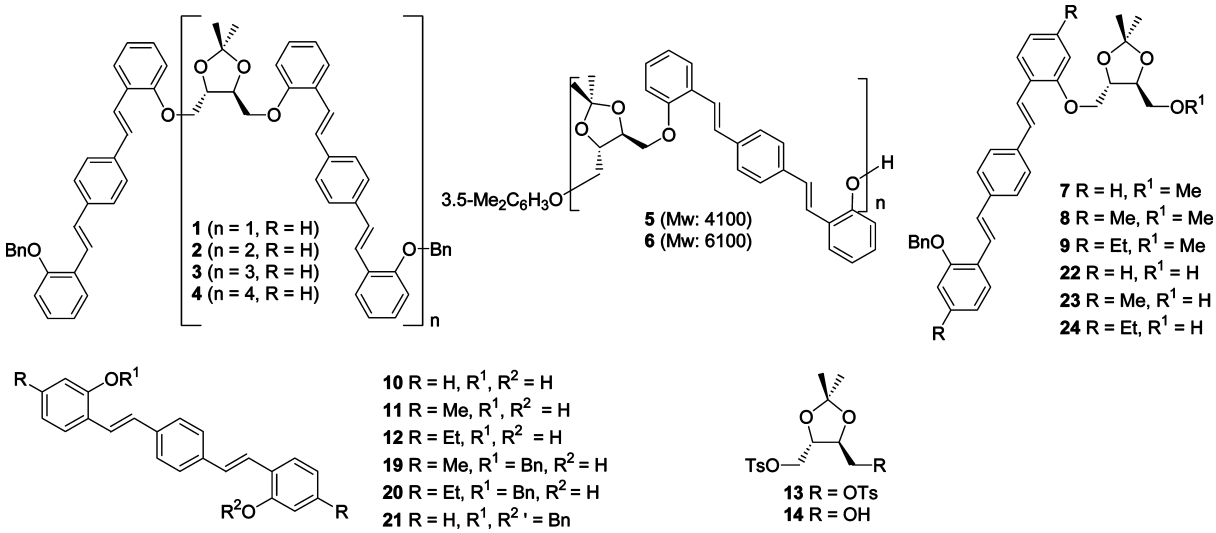

as β_M in eq 1),[13] that is inversely proportional to the molar fraction of the dopant (c), the cholesteric pitch (p, in μm), and the enantiomeric purity of the dopant (r)

$$\beta_M = 1/(pcr) \quad (1)$$

When several different kinds of chiral dopants are introduced, the contribution of each dopant on the helical twisting power can be described in a good additive approximation[5] as

$$(\beta_M)_{total} = \sum_i x_i(\beta_M)_i \quad (2)$$

where x_i is the mole fraction and $(\beta_M)_i$ is the HTP of the species i.[5] However, when chiral cores of a similar kind are positioned in different locations on a mesogenic skeleton, the chiral elements are carried into the LC matrix in different orientations. Under these situations, the HTP of the molecules may not obey the simple additive relationship and therefore their β_M cannot be predicted on the basis of the number of chiral centers on the molecule.[9d,14] A large variation of the HTP would be found for these compounds. For example, an elegant study of oligomeric binaphthols has been demonstrated recently in which the β_M does not follow the linear correlationship with the number of chiral units.[14a] Since we are interested in developing oligochiral dopants with predictable β_M, dopants with their chiral elements being aligned in a unique direction are highly desired. It is because their β_M is supposedly predictable on the basis of the additive relationship. In addition, the polychiral dopants must have good miscibility with the LC molecules in order to avoid phase segregation problems.

Herein we report the study of oligochiral dopants **1**−**9**, in which **2**−**6** obey the additive relationship (Scheme 1). This class of oligochiral dopants is derived from condensation of chiral 2,3-*O*-(isopropylidene)-L-threitol (L-(IPT)) with rigid-rod-like (*E,E*)-1,4-bis(styryl)benzene (BSB) moieties. The L-IPT is a C_2 chiral element that has chiral induction effect for cholesteric mesophases. BSB is a linear rigid component that determines mainly by the alignment order with the LC matrix and accordingly the chiral elements would be carried into the matrix in a specific direction. A model of cholesteric chiral induction by chiral *trans*-4,5-dimethyl-1,3-dioxolane derivatives has been reported in the literature[8] in which the chiral 1,3-dioxolane was aligned with its C_2 axis more or less parallel to the rodlike LC molecules; and the stereogenic fragment disturbed the parallel alignment and imposed the helicodial arrangement. Therefore, in our design, we adopted a flexible ether linkage to join the chiral 1,3-dioxolane and the rigid BSB elements so that the rigid-rod components are able to fold and align more or less parallel with the C_2 axis.

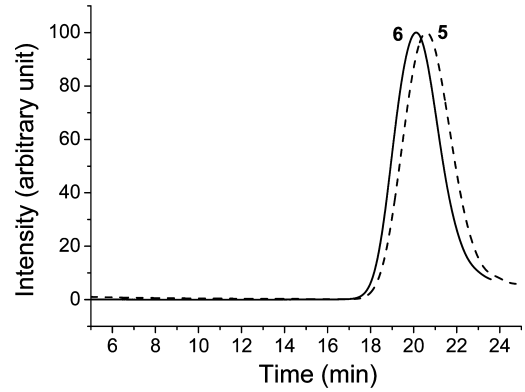

Figure 2. GPC diagram for oligomers **5** (M_w 4100) and **6** (M_w 6100).

Preparation of the Chiral Dopants. The synthetic precursors **10**−**14** used in the present works are shown in Scheme 1. While the oligomers **1**−**4** were synthesized by stepwise condensation, the polymers **5** and **6** were obtained in a one-pot condensation polymerization and end-capped with 3,5-dimethylphenol. In our work, (*E,E*)-1,4-bis(2′-hydroxystyryl)benzenes **10**−**12**,[15] L-IPT ditosylate (**13**),[16] and the monotosylate **14**[17] were adopted as the key building blocks for sequential condensation oligomerization and one-pot polymerization reactions. The one-pot condensation polymerization of **10** and **13** (1:1) was carried out in DMF in the presence of K_2CO_3 as base and substantially end-capped with 3,5-dimethylphenol. The polymer was purified by precipitation from MeOH three times to give **5**. The apparent M_w obtained by GPC (American Polymer Standard AM GPC Gel 10^4 Å 10 μm and 5 μm in serial) was 4100 against polystyrene standards (Figure 2). The number-average degree of polymerization (DP) of 10 was confirmed by using the ^{1}H NMR integration ratio between the dioxolane protons at δ 4.2−4.7 ppm and the terminal methyl protons at δ 2.2 ppm. Oligomer **6** with higher apparent M_w of 6100, with the DP of

SCHEME 2: Synthetic Sequence for Preparation of 1−4

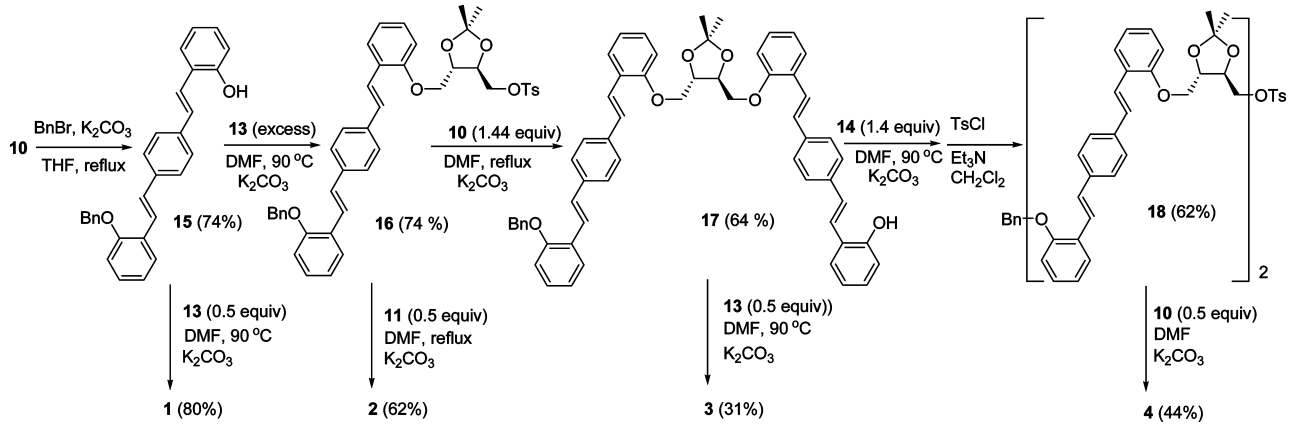

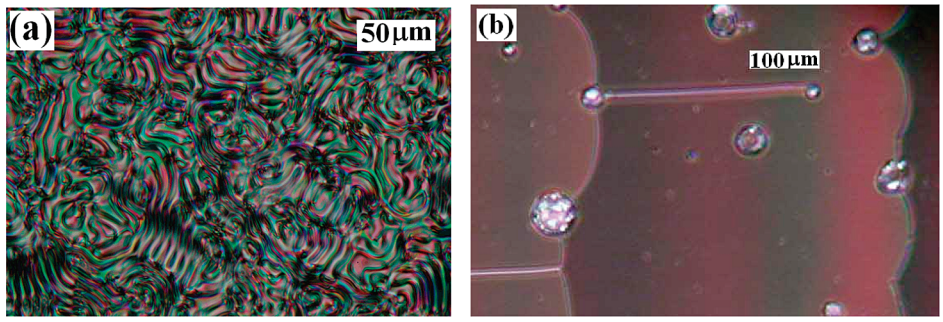

Figure 3. (a) Fingerprint texture of **5**-doped 5OCB. (b) An enlarged image of **6** doped 5OCB in a wedge cell at 50 °C. Phase separation zones were observed under a polarized microscope.

15 was isolated by using gel-permeation chromatography and THF as the eluent.

The synthetic procedures for oligomers **1**−**4** are shown in Scheme 2. Mono protection of **10** is done with a benzyl group to afford **15**, followed by condensation with 0.5 equiv of **13** to give **1** in 80% yield. When **15** was treated with excess amounts of **13**, monosubstituted dioxolane **16** was obtained in reasonable yield. By iterating the condensation strategy, **2** and **3** could successfully be obtained. However, a practical problem was faced when we applied this strategy for **4**. When **17** was treated with excess amounts of **13**, the desired **18** and the disubstituted **3** were simultaneously generated, which is difficult to separate. Therefore, our strategy was detoured so that **17** was first reacted with **14** to form the corresponding monoalcohol, followed by tosylation to give **18,** which was further coupled with **10** to give **4**. The monosubstituted dopants **7**−**9** were prepared in a similar stepwise sequence, in which **15**, **19**, and **20** were coupled with **14** to give **22**−**24**, respectively, followed by methylation to give **7**−**9**. The spectroscopic standard **21** was prepared through a one-step bis-benzylation of **10** under similar conditions.

Cholesteric Phase of Doped 4-Pentoxyl-4′-biphenylcarbonitrile (5OCB).[15] 5OCB is a nematic liquid crystal with a mesophase transition temperature (T_m) of 48 °C and isotropic phase transition temperature (T_i) of 68 °C. When **2**−**6** were doped, cholesteric fingerprint textures were observed, indicating that helical pitches were formed in the LC matrix (Figure 3). The left-turned helical handedness (−) was confirmed by contact experiments with *R*-(−) and *S*-(+)-2,2′-binaphthyl-1,1′-diol as the standards for comparison.[3a,9f,18] The observation of the left-turned helical handedness for the present L-**2**−**6** series (i.e., M twist for the L series) is complementary to that of reported by Spada for 2-aryl substituted (4*R*,5*R*)-dimethyl-1,3-dioxolanes **25**−**27** and D-threitol **28** in E7 (Figure 4), which show right-turned (P twist) helical handedness (i.e., P twist for the D series).[8]

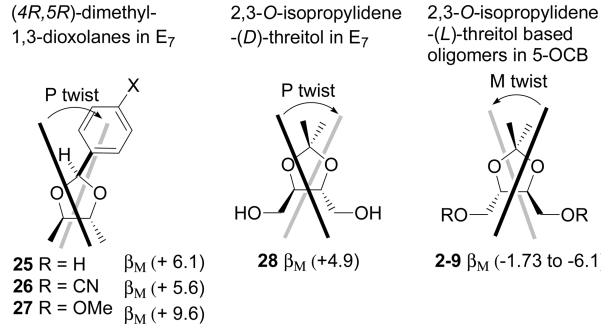

Figure 4. HTP (β_m) and handedness of the threitol derivatives. Note that P twist for the D-threitol was observed by Spada, which is consistent with the present results of M twist for the L-series.

These results imply the same chiral induction mechanism operating for either the C_2-chiral (4*R*,5*R*)-dimethyl-1,3-dioxolanes, D-IPT, or the present L-IPT series of **2**−**6**.

However, no fingerprint texture could be induced by **1** in 5OCB even at a high doping level of 21 wt %. The loss of the HTP of **1** in 5OCB suggested that not only the C_2-chiral dioxolane core but also the achiral BSB parts are responsible for the cholesteric behaviors. The effects of the BSB parts on the HTP will be discussed in a later paper.

The HTP of the chiral dopants are also quantified by Grandjean−Cano wedge experiments (using a cell from E.H.C., Japan), in which the induced pitch sizes at various dopant levels could be measured from the distance between the Grandjean−Cano disclination lines.[1,16] The chiral-induction capability of **2**−**5** in 5OCB was first compared as follows: for generation of the pitch size of 13 μm, the mole fractions of 0.0192, 0.0148, 0.0108, and 0.0042 for **2**−**5** were respectively required. The parameter of pitch/molar fraction (p/c) was then calculated as 680, 880, 1200, and 3100 μm for **2**−**5**. These results reflect the order of

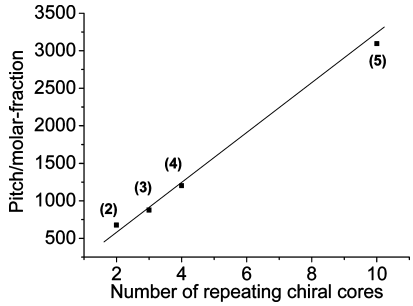

Figure 5. Plot of pitch/molar fraction at the pitch size of 13 μm versus the number of chiral L-threitol cores on the oligomers.

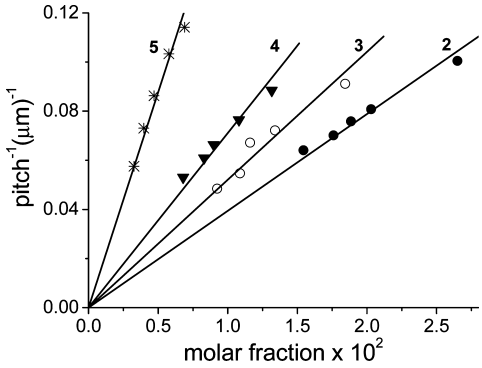

Figure 6. Inverse pitch (μm^{-1}) versus molar fraction of **2**−**5** in 5OCB, measured by using a Cano wedge cell at 50 °C.

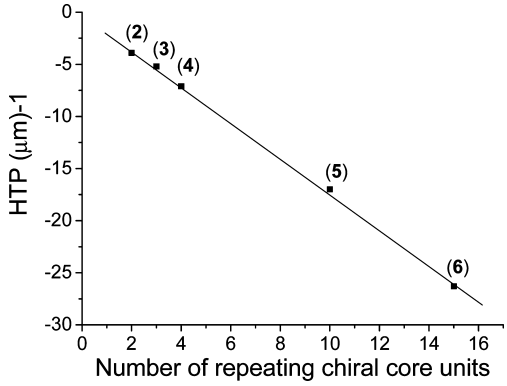

Figure 7. Correlation plot of the HTP versus the number of chiral L-threitol cores on the oligomers.

chiral-induction capability of **5** > **4** > **3** > **2**. A linear correlation plot of p/c versus the number of repeating chiral centers was observed in this case, implying that the capability of each chiral core on the pitch generation is essentially the same (Figure 5).

The quantitative parameter HTPs, defined as $\beta_M = 1/(pcr)$,[13] were calculated from the slope of a plot of $1/p$ versus the molar fraction (c) of the dopant, in which the enantiomeric purity (r) equals to 1 (Figure 6). All systems almost perfectly obeyed the linear relationship of $\beta_M = 1/(pcr)$ with the lines passing through the origin.

The β_M values obtained for **2**−**5** from the linear regression plots are −3.9, −5.2, −7.1, and −17.6 μm^{-1}, respectively, which are linearly proportional to the number of repeating chiral cores on the oligomers (Figure 7). Obviously, their β_M obeys the rule of summation of the HTP of each chiral unit. This could be rationalized by assuming that the chiral cores were orienting to the same axis so that their HTP could be maintained, without being canceled with each other due to orientation randomness. In order to further explore the limitation of the linear relationship, another polymeric sample of **6,** with an higher number average DP of 15, was prepared by GPC for study. As shown in Figure 7, **6** also obeys the linear relationship and shows β_M of −26.3 μm^{-1}, which could be reduced to 1.75 μm^{-1} per chiral core. However, small amounts of white and bubblelike phase segregation domains were found in the sample (Figure 3b). The presence of these domains in the cholesteic planar texture lowered the clearing point locally and caused some disorder of the disclination line. We attributed these to the phase-segregation phenomenon that is due to the lower miscibility of the high molecular weight portions in the liquid crystal.

Temperature Dependence Experiments. The temperature dependence of the pitch of the cholesteric phase is of particular importance for certain LC applications.[19] In dopant induced cholesteric liquid crystals, both an increase and a decrease of the pitch with temperature and even helix inversions have been observed. The HTP (β_M) of a given dopant in a nematic LC could be expressed as $\beta_M = (RT\varepsilon)Q/2\pi K_{22}\nu\mu_m$, where ε is the orienting strength of the LC environment, R is the gas constant, T is the absolute temperature, K_{22} is the twist elastic constant, ν_m is the molar volume of the solution, and Q is the chirality parameter which is governed by the coupling of chirality and orientational behavior of the dopant.[8,10,20] The definition of Q could be expressed by $Q = -(2/3)^{1/2}(Q_{xx}S_{xx} + Q_{yy}S_{yy} + Q_{zz}S_{zz})$, where $S_{\zeta\zeta}$ are the principal elements of the Saupe ordering matrix **S** and $Q_{\zeta\zeta}$ is the corresponding component of the helicity tensor **Q**. Therefore, several factors that operate in opposite trends may be responsible for the temperature dependence of the helical twist, among which variation of order ($S_{\zeta\zeta}$) of the nematic molecules, of the elastic response (K_{22}) of the helical twist, and of conformational population redistribution which is related to Q are essential for the phenomena. When temperature increases, the elastic response (K_{22}) of the LC matrix would become weak, and therefore reduction of the K_{22} would amplify the effect of the chiral dopants on the helical twist. The $d\beta_M/dT$ would therefore be positive. On the other hand, the increase of temperature is accompanied by an increase in the dynamic conformational disorder, leading to an overall weakening of the twisting power of the dopant molecules. Under this situation, the $d\beta_M/dT$ would be negative. From the structural points of view, the HTP of a chiral dopant would be governed by the order effect and the porter effect. The dependence of the HTP on the order of the guest and the host is known as the order effect. However, chiral groups substituted on an achiral skeleton possess a distinct orientational order in the liquid crystal phase, which depends on the order of the skeleton. This effect is known as the porter effect. Although the HTP is arising from the contributions of all conformers of the chiral dopant, helical conformers are expected to be the origin of the HTP effect. When the temperature varies, redistribution of the population of the different conformers would lead to a change of the HTPs. In our cases, the order effect is controlled by the C_2-chiral L-threitol cores while the porter effect is coming from the rigid BSB components. Indeed, contributions of different sign and magnitude to the HTP can be derived from different parts in the molecule. About the (4*R*,5*R*)-dimethyl-1,3-dioxolane systems, it was evidenced that the nematic molecules would align along with the C_2 axis (Figure 4). P twist of the chiral nematics would lead to a positive sign (+) while M twist would lead to a negative sign (−). In our system, observation of the negative β_M for **2**−**9** suggested the M helicity along the C_2 axis of the chiral L-IPT cores.

Again, as shown in Figure 8, the consistent decreasing trends of the β_M versus temperature for **2**−**7** suggested that the chirality transmission mechanisms for the whole series of dopants are

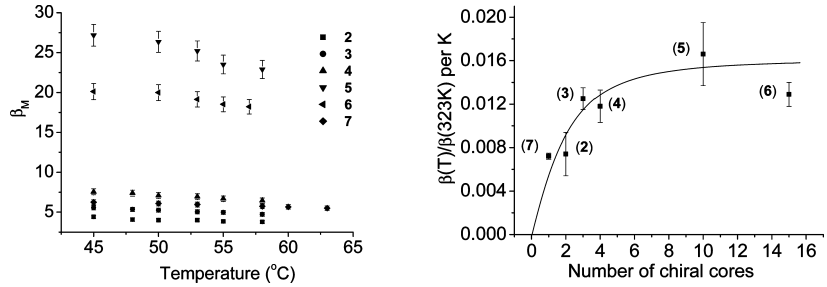

Figure 8. (a, left) Decreasing trends of the β_M versus temperature. (b, right) The molecular weight dependency of the temperature susceptibility of $\beta_M(T)/\beta_M(323\ K)$.

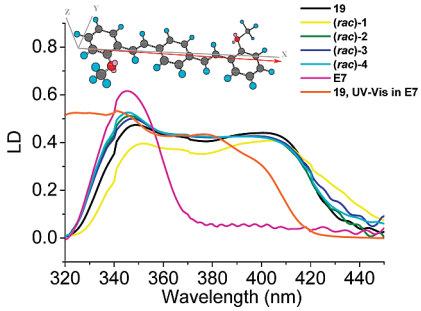

Figure 9. Linear dichromism of the racemic chiral dopants in E7. Inset diagram shows the orientaion of the transition dipole moment of the BSB segment. The orange line shows the UV−vis absorption spectrum of a thin-liquid film of **19** in E7 as reference for comparison.

similar. As the temperature increases, the HTP in all plots decreases due to the conformational disorder, leading to negative slopes in Figure 8a. However, the temperature susceptibility of the normalized HTP, defined as $\beta_M(T)/\beta_M(323\ K)$ per K, is found to be slightly molecular weight dependent (Figure 8b). As shown in Figure 8b, the macromolecular dopants would show stronger temperature susceptibility than the small molecular dopants. The temperature susceptibility increases from 0.0073 ± 0.0001 for **2** and **7,** and reaches to a plateau of 0.015 ± 0.002 at high molecular weight region.

Linear Dichromism (LD) in the Anisotropic Phase. Although linear dichromism (LD) is a common method to provide information about the alignment of the dopants in the LC matrix.[9a,b] it was difficult to extract useful information about the alignment of the C_2-threitol chiral cores due to the lack of the appropriate chromophores in our cases. In addition, the small HTP value of the oligomers indicates that the interactions between the chiral cores and the host-nematic LC might be small. Nevertheless, the LD experiments would allow us to understand the relative orientation of the rigid BSB segments with respect to the director of the nematic environment. In order to carry out the measurement at room temperature, a commercially available room temperature liquid crystal named as E7,[8a] instead of 5OCB,[8a] was adopted in these experiments. Antiparallel rubbed polyimide coated ITO LC cells[21] were employed in order to restrict the orientation of the nematic director. The alignment of the nematic liquid crystal could be confirmed by the LD experiment. As shown in Figure 9, only slightly red-shifted spectrum of **1**−**5** in E7, in comparison to that of **19**, was observed, indicating that the electronic $\pi-\pi$ interactions between BSB and E7 are weak. When the mixed polarizations are small, a relationship linking the LD to the Saupe order parameter (S_{uu}) could be expressed as $LD = (\varepsilon_{||}(\lambda) - \varepsilon_{\perp}(\lambda))/(\varepsilon_{||}(\lambda) + \varepsilon_{\perp}(\lambda)) = 3S_{uu}/(2 + S_{uu})$, where $\varepsilon_{||}(\lambda)$ and $\varepsilon_{\perp}(\lambda)$ are the optical densities of the two perpendicularly plane-polarized components of the incident radiation and the reduced linear dichromism is denoted as LD.

Since the absorption regions of E7 (345 nm) and BSB (375 nm) segments are well resolved (Figure 9), the LD signals from these two independent components could be directly observed. In order to evaluate the orientation of the BSB segments with respect to the E7 molecules, the orientation of the transition dipole of (*E*,*E*)-4,4′-bis(2-methoxystyryl)benzene, a model compound, was first calculated by AM1 and ZINDO.[22] The result is shown in the inset of Figure 9. By comparing the LD signals of the BSB segments against that of E7, the relative orientation of the BSB segment with respect to the director of E7 could be estimated.

The LD experiments were performed in E7 using racemic **1**−**5** as dopants, which were prepared by equally mixing the L-**1**−**5** with their D-enantiomers. Pure E7 shows LD band at 340 nm while two positive and broad LD bands at 340 and 405 nm were observed for the (*rac*)-**1**−**5** in E7. The spectral range of the LD matches quite well with the corresponding UV absorption spectrum of the BSB chromophore and E7. While the LD band at 340 nm is assigned to the electronic $\pi-\pi^*$ transition of E7, the band at 405 nm corresponds to the electronic $\pi-\pi^*$ transition of the BSB segments. However, the spectral shape of the band at 405 nm was slightly distorted due to the anisotropic effects of the aligned nematic environments. Since the value of $LD = 3S_{uu}/(2 + S_{uu})$ is a function of the orientation parameter, the comparable LD of 0.42 ± 0.02 for (*rac*)-**2**−**5** at 405 nm, and of 0.52 ± 0.03 for E7 at 347 nm, indicated that their long axes of the BSB segments are more or less parallel to the director of the E7.

On the other hand, (*rac*)-**1** in E7 shows lower LD of 0.38 at 340 nm, indicating that the nematic alignments are less ordered when dopant **1** was added. This observation is consistent with the results of our previous experiment, in which no cholesteric phase could be generated in L-**1** doped 5OCB.

To further understand the behavior of oligochiral dopants **2**−**6**, we adopted **7**−**9** as references to study. Perhaps the same chiral dioxolane cholesteric phase induction mechanism is operating in all these cases; their HTPs (β_M/core) and handedness were found to be −6.1, −3.8, and −3.3, which are very close to those of **2**−**6**. However, small but observable porter effects were recorded among **7**−**9**. For **7** with the BSB unsubstituted, stronger HTP (β_M/core) of −6.1 was observed. On the other hand, when the BSB segments are methyl or ethyl substituted, **8** and **9** showed HTP (β_M/core) of −3.8 and −3.55 that are more close to those of **2**−**6**. Since the alkyl-substituted BSB segments have larger length/diameter aspect ratios, we expect that **8** and **9** are more mesogenic and would have better alignment with the nematic matrix. Therefore, we conclude that stronger alignment of the BSB unit with the nematic matrix would lead to lower value of the β_M/core. Of course, increasing the number of repeating units on the oligomeric dopants is essential to provide larger driving force for the alignment. Therefore, it is

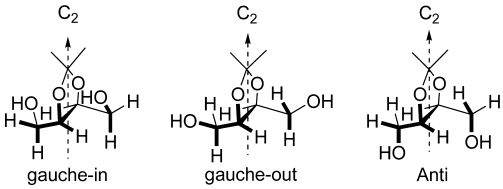

Figure 10. Conformational analysis of 2,3-*O*-(isopropylidene)-L-threitol.

no surprise that when the number of the repeating units increases, the HTP (β_M/core) approaches the limit value of −1.7.

Models for the Cholesteric Phase Induction. During the past few decades, models for the chirality transmission from a chiral dopant to the bulk of the nematic solvent have been extensively investigated, in which the chiral dopants are assumed to act as templates to select chiral conformations of the LC molecules lying next by them and therefore induce chiral conformation in the nearest-neighbor molecules. The induced chirality in this layer would then be passed to the next layer through similar mechanisms and so on to the neighbor. On the basis of this model, a chiral induction mechanism for (4*R*,5*R*)-dimethyl-1,3-dioxolanes has been established by Spada. In this model, the dioxolane dopant is aligned with its long axis more or less parallel to the rodlike LC molecules (Figure 4). However, the (4*R*,5*R*)-stereogenic fragment disturbs the parallel alignment and imposes the P-twist helicoidal arrangement.[2b] This kind of model has been applied for other systems in the past.[23] Although the chiral induction mechanism for D-threitol has not been deeply explored, Spada obtained a similar β_M in the measurement with the same helical twist handedness. These results reflected that the chiral induction mechanisms for (4*R*,5*R*)-dimethyl-1,3-dioxolanes and D-threitol are alike. Although theoretical calculations about the conformational structures of the chiral cores in the gas phase may not be accurate enough to explain all observations and phenomena in nematic liquid crystals due to their small difference in energies as well as the perturbation arising from the ordered host matrix, it might be still useful for providing some insights about their relative conformational stabilities. Since we adopted L-threitol as the chiral component in our systems, PM5 calculations[24] for L-threitol had been performed, in which three possible C_2-chiral conformations, which are shown in Figure 10, were identified. The first one is the gauche-in conformation with the OH groups inclining to the C_2 molecular axis. The second one is the gauche-out conformation with the OH groups turning outward. The third one is the anti conformation with the OH groups anti to the dioxolane oxygens. Among them, the calculated heats of formation of the gauche-in (−195.5 kcal/mol) and gauche-out (−195.2 kcal/mol) conformations are almost identical but about 3 kcal/mol lower than that of the anti conformation (−192.5 kcal/mol). Therefore, the anti conformer should be the least important for the chiral induction. On the other hand, the gauche-out conformer should be the most significant one. Generally speaking, chiral induction relies on the short-range intermolecular interactions. Since the nematic molecules are kept off from the C_2-axis in the gauche-in conformation by the −OH groups, small chiral-induction effect is expected. On the other hand, the gauche-out conformation has a C_2 chiral environment similar to that of **20**−**22**. Therefore, it is easy to perceive that the gauche-out conformation would be the key conformation for the M-twist chiral-induction mechanisms.

On the other hand, conformational analysis for the less rigid **7** is more complicated. To simply our calculation, the terminal −OBn group was replaced by hydrogen for clarity. Our calculations showed that there are at least three possible conformers, denoted as (a)−(c), respectively, when viewed along the C−O bond. The corresponding Newman projections are shown in Figure 11. Unlike conformer (a), with the BSB matches well with the M-twist liquid crystal alignment, conformers (b) and (c) should be less important due to the mismatching orientation of the rodlike BSB fragment. Therefore, we propose that the M-helical twist is originating from conformer (a).

On the basis of the above discussion, a model for the oligomeric structure could be built as illustrated in Figure 12, in which the conformation of **7** is repeatedly extended. Our model was built on the basis of several assumptions. (1) Spada's model about the alignment of the nematic LC molecules with repsect to the C_2-chiral dioxolane core is still valid. This assumption we made is based on the fact that all molecules have the same handedness of the cholesteric phases that matches well with Spada's model. (2) The BSB segments are aligned more or less parallel to C_2-chiral axis. The second assumption is based on the results of the linear dichroism experiments, in which the LD for the BSB segments is close to that of the E7 molecules. (3) All repeating units favor alignment on the same axis, named as the *Z*-axis in our diagram. This assumption is based on the additivity relationship, in which the β_M/core values for **8**, **9,** and the oligomers are almost identical. (4) The local environment of each L-threitol core should maintain the C_2-chiral symmetry. This is because the helical conformers are expected to be the origin of the HTP effect.

On the basis of this model, one could easily illustrate and explain why the dopant favors to have the M-helical twist in a nematic solvent as well as the origins of the linear β_M and number of the repeating chiral cores correlationship.

In summary, we provided a strong proof for the HTP addition rule of oligomeric and polymeric chiral dopants having the C_2-chiral cores chained alternatingly with rigid segments. This family of dopants shows good miscibility with nematic liquid crystals so that high molecular weight dopants could be tolerated without significant phase segregation. The HTP of this family obeys the addition rule so that the molar HTP is linearly proportional to the number of repeating units. This observation is highly exciting because the HTP per core could still be maintained, no matter whether the cores are evenly spread in a form of monomer in the LC matrix or being tightly confined in a polymer. The designs of the next generation of dopant with higher miscibility with nematic liquid crystals are ongoing.

Experimental Section

General Information. Tetrahydrofuran (THF) was distilled from Na under N_2, using benzophenone as indicator. Dimethylformamide (DMF) was dried with activated molecular sieves (4 Å) and distilled before use. All other reagents and solvents were of analytical or chemical grade or were purified using standard methods. The wedge cells were ordered from E.H.C. Japan, with the uncertainty of ±5% on the value of tan θ.

1,4-(*E*,*E*)-Bis(2-hydroxystyryl)benzene Monobenzyl Ether (15) Typical Procedure. To a solution of **10** (0.21 g, 0.65 mmol) in THF (1 mL) was added under N_2 anhydrous K_2CO_3 (0.48 g, 3.5 mmol). The mixture was refluxed for 10 min, followed by addition of benzyl chloride (0.082 g, 0.65 mmol) in THF (1 mL). The reaction mixture was further refluxed for 24 h, and quenched with aqueous HCl (1 N) after cooling to room temperature. The crude solid precipitated from the solution were collected by filtration and purified by flash chromatography on silica gel (toluene) to give yellow crystals (0.20 g, 0.48 mmol, 74%): mp 142−143 °C; ^{1}H NMR (300 MHz, DMSO-d_6) δ 9.77

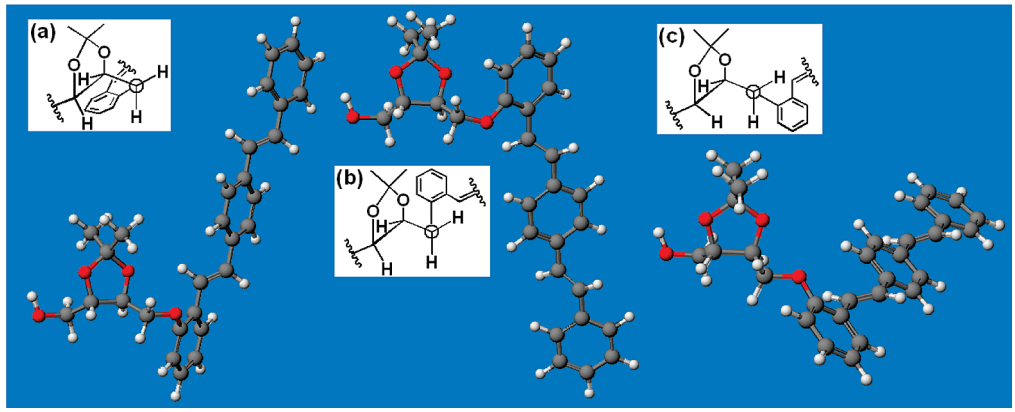

Figure 11. Conformational analysis for a simplified **19**. The terminal −OBn group was removed in order to simplify the PM5 computation.

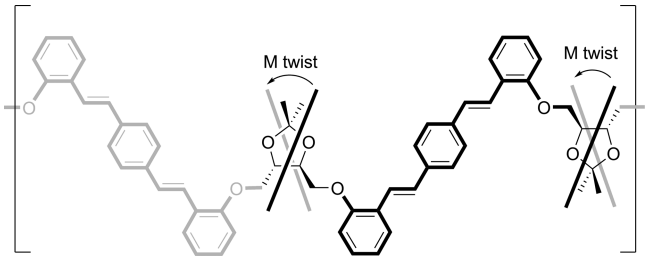

Figure 12. Molecular model for the conformations of the oligochiral dopants of **2**−**6** in 5-OCB and E7. The crossed bars represent the orientation of the nematic layers above and under the chiral units.

(s, 1 H), 7.68 (d, J = 7.4 Hz, 1 H), 7.57−7.11 (m, 17 H), 6.98 (t, 1 H), 6.36 (m, 2 H), 5.23 (s, 2 H); ^{13}C NMR (100 MHz, $CDCl_3$) 156.2, 153.0, 137.4, 137.2, 136.7, 129.9, 128.9, 128.6, 127.9, 127.3, 127.2, 126.9, 126.85, 126.83, 126.7, 124.8, 123.5, 122.6, 121.2, 121.2, 115.9, 112.8, 70.5; MS m/z FAB (NBA) 404.2; HRMS (M^+) calcd for $C_{18}H_{24}O_2$ 404.1776; found 404.1779.

1,4-(*E*,*E*)-Bis(2-hydroxy-4-methylstyryl)benzene Monobenzyl Ether (19). The monobenzyl ether was prepared from **11** according to the typical procedure with the yield of 50.6%. mp 135−137 °C; ^{1}H NMR (400 MHz, DMSO-d_6) δ 9.65 (s, 1H), 7.16 (d, J = 16 Hz, 1H), 7.10 (d, J = 16 Hz, 1 H), 7.22−7.11 (m, 2 H), 6.97 (s, 1 H), 6.80 (d, J = 8.0 Hz, 1 H), 6.68 (s, 1 H), 6.63 (d, J = 8.0 Hz, 1 H), 5.19 (s, 2 H), 2.31 (s, 3 H), 2.23 (s, 3 H); ^{13}C NMR (100 MHz, DMSO-d_6) δ 155.31, 154.61, 138.34, 138.02, 137.03, 136.76, 136.18, 128.30, 127.61, 127.53, 127.23, 126.34, 126.28, 126.17, 126.11, 123.27, 122.97, 122.49, 121.53, 120.87, 120.06, 116.16, 113.56, 69.57, 21.30, 21.01; HRMS (FAB) calcd for $C_{31}H_{28}O_2$ 432.2089; obsd 432.2085.

1,4-(*E*,*E*)-Bis(2′-hydroxy-4′-ethylstyryl)benzene Monobenzyl Ether (20). The monobenzyl ether was prepared from **12** according to the typical procedure with the yield of 53.9%; mp 154−155 °C; ^{1}H NMR (400 MHz, $CDCl_3$) δ 7.53−7.30 (m, 13 H), 7.10 (d, J = 16 Hz, 1 H), 7.05 (d, J = 16 Hz, 1H), 6.82 (d, J = 8.0 Hz, 1 H), 6.79 (s, 1 H), 6.78 (d, J = 8.0 Hz, 1 H), 6.65 (s, 1 H), 5.14 (s, 2 H), 2.66−2.57 (m, 4 H), 1.25−1.21 (m, 6 H); ^{13}C NMR (100 MHz, $CDCl_3$) δ 155.92, 152.88, 145.17, 145.05, 137.06, 137.04, 136.59, 128.45, 128.39, 127.88, 127.70, 127.20, 126.75, 126.53, 126.50, 126.38, 124.22, 123.10, 122.55, 121.96, 120.57, 120.51, 115.31, 112.40, 70.55, 29.06, 28.59, 15.58, 15.42; HRMS (FAB) calcd for $C_{33}H_{32}O_2$ 460.2402; obsd 460.2397.

***p*-Toluenesulfonyl-4-*O*-{(2-(*E*)-{4-[2-(2-benzyloxyphenyl)-(*E*)-vinyl]phenyl}vinyl)phenyl}-2,3-*O*-isopropylidene-L-threitol (16).** To an oven-dried double-necked flask were charged **15** (2.8 g, 6.9 mmol), **13** (6.49 g, 13.8 mmol), K_2CO_3 (4.77 g, 34.5 mmol) and DMF (7 mL). The reaction mixture was reacted at 90 °C under N_2 for 3.5 h. After being cooled to room temperature, the reaction mixture was diluted with chloroform (20 mL) and filtered. The collected filtrate was washed with water. The aqueous layer was re-extracted with chloroform (2 × 20 mL). The extracts were collected, dried over anhydrous $MgSO_4$, concentrated and purified by flash chromatography on silica gel (toluene/ethyl acetate) to give **16** yellowish viscous glassy solid (3.9 g, 5.1 mmol, 74%); $[\alpha]^{25.0}_D$ = +1.00 (c = 1.00, CH_2Cl_2); ^{1}H NMR (300 MHz, $CDCl_3$) δ 7.74 (d, J = 8.2 Hz, 2 H), 7.64−7.60 (m, 2 H), 7.56 (d, J = 16.6 Hz, 1 H), 7.48−7.13 (m, 15 H), 7.12 (d, J = 7.4 Hz, 1 H), 7.02−6.94 (m, 3 H), 6.87 (d, J = 8.1 Hz, 1 H), 5.16 (s, 2 H), 4.27 (m, 4 H), 4.13 (m, 2 H), 2.33 (s, 3 H), 1.44 (s, 3 H), 1.39 (s, 3 H); ^{13}C NMR (100 MHz, $CDCl_3$) δ 156.1, 155.6, 145.0, 137.3, 137.1, 136.9, 132.6, 129.9, 129.1, 128.9, 128.61, 128.57, 127.90, 127.88, 127.23, 126.94, 126.91, 126.87, 126.85, 126.6, 126.4, 123.4, 122.7, 121.6, 121.2, 112.8, 112.4, 110.6, 77.2, 76.2, 75.7, 70.5, 69.0, 68.3, 27.0, 26.9, 21.5; HRMS (M^+) calcd for $C_{43}H_{42}O_7S$ 702.2651; found 702.2661.

Compound 1. (A Typical Coupling Procedure for 2−4). To a double-necked flask were charged **15** (0.28 g, 0.70 mmol), **13** (0.18 g, 0.38 mmol), anhydrous K_2CO_3 (0.24 g, 1.75 mmol), and DMF (1 mL). The mixture was reacted at 90 °C for 16 h under N_2. The resulting mixture was subsequently quenched with water and extracted with ethyl acetate (3 × 20 mL). The organic extracts were collected, washed with saturated brine, dried over anhydrous $MgSO_4$, concentrated by rotary evaporator, and purified by flash chromatography on silica gel (toluene) to give **1** as yellowish solid. (0.26 g, 0.28 mmol, 80%): mp 120−125 °C $[\alpha]^{25.5}_D$ = +18.98 (c = 1.36, CH_2Cl_2). ^{1}H NMR (500 MHz, acetone-d_6) δ 7.67−7.64 m, 4H), 7.59 (d, J = 7.6 Hz, 2 H), 7.56−7.54 (m, 6 H), 7.49 (d, J = 8.3 Hz, 4 H), 7.44−7.40 (m, 8 H), 7.36−7.33 (m, 2 H), 7.28−7.18 (m, 8 H), 7.11 (d, J = 8.4 Hz, 2 H), 7.08 (d, J = 8.3 Hz, 2 H), 6.99−6.95 (m, 4 H), 5.24 (s, 4 H), 4.68 (s, 2 H), 4.42 (s, 4 H), 1.53 (s, 6 H); ^{13}C NMR (125 MHz, $CDCl_3$) δ 156.12, 155.73, 137.15, 137.07, 136.87, 129.07, 128.94, 128.61, 128.53, 127.91, 127.30, 126.94, 126.91, 126.80, 126.72, 126.59, 126.46, 123.22, 122.80, 121.53, 121.13, 112.70, 112.35, 110.24, 77.08, 70.49, 69.00, 27.17; HRMS (M^+) calcd for $C_{65}H_{58}O_6$ 934.4233; found 934.4238. Anal. Calcd for $C_{65}H_{58}O_6$: C, 83.48; H, 6.25; O, 10.27. Found: C, 83.65; H, 5.95.

Compound 2. Compound **10** (0.062 g, 0.20 mmol), **16** (0.25 g, 0.36 mmol), anhydrous K_2CO_3 (0.124 g, 0.897 mmol), and DMF (0.5 mL) were reacted at 90 °C for 16 h under N_2 to give the crude **2** that was purified by flash chromatography on silica gel (PhMe:EtOAc = 1:1) to give essentially pure **2** as yellow

solid (0.153 g, 0.112 mmol, 62%): mp 110−115 °C; $[\alpha]^{25.5}_D$ = +25.0° (*c* = 1.02, CH_2Cl_2). ^{1}H NMR (400 MHz, $CDCl_3$) δ 7.80−7.65 (m, 10H), 7.60−7.57 (m, 6 H), 7.52−7.45 (m, 17 H), 7.27−7.07 (m, 21 H), 7.07−6.90 (m, 4H), 5.23 (s, 4H), 4.65 (s, 4 H), 4.39−4.31 (m, 8 H), 1.69 (s,6H), 1.68 (s, 6H); ^{13}C NMR (125 MHz, $CDCl_3$) δ 156.11, 155.76, 155.71, 137.14, 137.06, 136.90, 136.85, 129.11, 129.07, 128.94, 128.67, 128.61, 128.54, 127.91, 127.30, 126.93, 126.88, 126.81, 126.74, 126.72, 126.59, 126.53, 126.44, 123.22, 122.86, 122.77, 121.51, 121.13, 112.69, 112.35, 110.25, 76.88, 70.47, 69.01, 27.17; MS *m/z* FAB (NBA) 1375.6. Anal. Calcd for $C_{94}H_{86}O_{10}$: C, 82.07; H, 6.30; O, 11.63. Found: C, 81.82, H, 6.17.

1-[*O*-2-(2-(*E*)-{4-[2-(*E*)-(2-Hydroxyphenyl)vinyl]phenyl}-vinyl)phenyl]-4-[*O*-2-(2-(*E*)-{4-[2-(*E*)-(2-benzyloxyphenyl)vinyl]phenyl}vnyl)phenyl]-2,3-[*O*-isopropylidene]-L-threitol (17). Compound **10** (0.354 g, 1.13 mmol), **16** (0.549 g, 0.78 mmol), anhydrous K_2CO_3 (0.604 g, 4.37 mmol) in DMF (1.5 mL) were reacted at 90 °C for 19 h under N_2. The resulting mixture was subsequently quenched by aqueous HCl (1 N) and extracted with EtOAc (3 × 20 mL). The organic extract was collected, washed with brine (saturated), dried over anhydrous $MgSO_4$, and concentrated. The crude mixture was purified by flash chromatography on pretreated silica gel (3% triethylamine in hexane), using PhMe/EtOAc (1:1) as eluent to give **17** as yellowish viscous oil. (0.409 g, 0.50 mmol, 64%): mp > 170 °C dec $[\alpha]^{25.8}_D$ = +15.20 (*c* = 1.00, CH_2Cl_2). ^{1}H NMR (300 MHz, $CDCl_3$) δ 7.65−7.25 (m, 21 H), 7.22−6.87 (m, 15 H), 6.78 (d, *J* = 8.1 Hz, 1 H), 5.30 (bs, 1 H), 5.17 (s, 2 H), 4.58 (s, 2 H), 4.30 (m, 4 H), 1.59 (s, 6 H); ^{13}C NMR (100 MHz, $CDCl_3$) δ 156.1, 155.7, 153.0, 137.1, 137.1, 137.0, 136.8, 136.7, 129.5, 129.1, 129.0, 128.9, 128.7, 128.6, 128.5, 127.9, 127.3, 127.0, 126.9, 126.83, 126.78, 126.7, 126.6, 126.4, 124.7, 123.2, 122.9, 122.8, 122.7, 121.5, 121.1, 121.0, 115.9, 112.7, 112.4, 112.3, 110.3, 77.05, 70.5, 69.0, 68.9, 27.2; HRMS (M^+) calcd for $C_{58}H_{52}O_6$ 844.3764; found 844.3764.

Compound 3. Compound **10** (0.145 g, 0.308 mmol), **13** (0.580 g, 0.686 mmol) anhydrous K_2CO_3 (0.094 g, 0.680 mmol) in DMF (0.5 mL) were reacted at 90 °C under nitrogen for 48 h to give a crude mixture that was purified by flash chromatography on silica gel (PhMe:EtOAc = 1:1) to give **3** as yellow solid. (0.196 g, 0.095 mmol, 31%). The compound could be further recrystallized from EtOAc−hexanes to afford analytical sample: mp 110−115 °C; $[\alpha]^{26.7}_D$ = +25.63 (*c* = 0.96, CH_2Cl_2).^{1}H NMR (400 MHz, $CDCl_3$) δ 7.30−7.55 (m, 40 H), 6.82−7.12 (m, 34 H); 5.14 (s, 4 H), 4.53 (s, 6 H), 4.30−4.21 (m, 12 H), 1.53(s, 6 H), 1.52 (s, 6 H), 1.51 (s, 6 H); ^{13}C NMR (125 MHz, $CDCl_3$) δ 156.11, 155.78, 155.74, 155.71, 137.14, 137.06, 136.88, 136.85, 129.11, 129.07, 128.93, 128.67, 128.61, 128.54, 127.91, 127.30, 126.91, 126.81, 126.75, 126.72, 126.59, 126.53, 126.44, 123.22, 122.84, 122.77, 121.51, 121.13, 112.69, 112.34, 110.25, 76.88, 70.5, 69.0, 27.2; MS *m/z* FAB(NBA) 1815.8. Anal. Calcd for $C_{123}H_{114}O_{14}$: C, 81.34; H, 6.33; O, 12.33. Found: C, 81.04; H, 6.08.

Two-Step Synthetic Sequence for Preparation of 18 from 17. Compound **14** (0.276 g, 0.873 mmol), **17** (0.615 g, 0.728 mmol), and anhydrous K_2CO_3 (0.503 g, 3.640 mmol) in DMF (1.0 mL) were reacted at 90 °C for 12 h under N_2. To secure that the conversion was complete, additional amounts of **14** (0.060 g, 0.190 mmol) were added and reacted for another 30 h. The resulting mixture was finally quenched with water. The product was extracted with EtOAc (3 × 30 mL). The collected organic extracts were washed with saturated aqueous NaCl, dried over anhydrous $MgSO_4$ and concentrated. The crude product was purified by flash chromatography on silica gel (PhMe/EtOAc = 1:1) to give the monosubstituted threitol intermediate as yellowish glassy solid. (0.453 g, 0.459 mmol, 63%): $[\alpha]^{25.8}_D$ = +24.95 (*c* = 1.01, CH_2Cl_2);^{1}H NMR (400 MHz, $CDCl_3$) δ 7.61− 7.46 (m, 9H), 7.42−7.34 (m, 12 H), 7.23−7.02 (m, 8 H), 7.02−6.85 (m, 8 H), 5.16 (s, 2 H), 4.55−4.54 (m, 2 H), 4.31−4.11 (m, 8 H), 3.92 (m, 1 H), 3.76 (m, 1 H), 1.95 (bs, OH), 1.55 (s, 3 H), 1.54 (s, 3 H), 1.47 (s, 6 H); ^{13}C NMR (100 MHz, $CDCl_3$) δ 156.1, 155.8, 155.7, 137.16, 137.09, 137.06, 136.92, 136.88, 129.16, 129.11, 129.07, 128.96, 128.73, 128.64, 128.58, 127.95, 127.34, 126.95, 126.93, 126.82, 126.75, 126.62, 126.54, 126.50, 123.25, 123.00, 122.78, 121.56, 121.16, 112.72, 112.42, 112.37, 112.33, 110.28, 109.77, 79.30, 76.84, 75.30, 70.51, 69.04, 68.94, 68.72, 62.14, 27.20, 27.16, 27.09; HRMS (M^+) calcd for $C_{65}H_{64}O_9$ 988.4550; found 988.4563. The monosubstituted threitol intermediate (0.394 g, 0.398 mmol) was further tosylated by reaction with *p*-toluenesulfonyl chloride (0.135 g, 0.764 mmol) in CH_2Cl_2 (0.6 mL) at 0 °C for 1.5 h, using Et_3N (0.3 mL) as the catalyst and acid scavenger. The resulting mixture was quenched with aqueous HCl (1 N) and extracted with EtOAc (3 × 30 mL). The organic extract was combined, washed with saturated brine, dried over anhydrous $MgSO_4$, concentrated, and purified by flash chromatography on silica gel (toluene/ethyl acetate) to give **18** as yellow glass. (0.450 g, 0.394 mmol, 99%): $[\alpha]^{25.8}_D$ = +17.60 (*c* = 1.00, CH_2Cl_2); ^{1}H NMR (400 MHz, $CDCl_3$) δ 7.72 (d, *J* = 8.3, 2 H), 7.62−7.32 (m, 22 H), 7.23−7.03 (m, 16 H), 6.87 (d, *J* = 8.2, 1 H), 6.86 (d, *J* = 8.2, 2H), 5.16 (s, 2 H), 4.55 (m, 2 H), 4.31−4.14 (m, 8 H), 4.14 (m, 2 H), 2.31 (s, 3 H), 1.55 (s, 3 H), 1.54 (s, 3 H), 1.42 (s, 3 H), 1.38 (s, 3 H); ^{13}C NMR (100 MHz, $CDCl_3$) δ 156.10, 155.76, 155.70, 155.56, 145.02, 137.12, 137.06, 136.80, 132.50, 129.9, 129.16, 129.05, 129.02, 128.91, 128.71, 128.67, 128.61, 128.55, 128.21, 127.91, 127.3, 126.91, 126.89, 126.86, 126.81, 126.71, 126.57, 126.52, 126.46, 126.42, 123.21, 122.96, 122.75, 122.60, 121.61, 121.51, 121.49, 121.12, 112.67, 112.34, 112.32, 110.56, 110.23, 77.21, 76.79, 76.14, 75.67, 70.45, 68.99, 68.89, 68.24, 27.15, 27.02, 26.85, 21.56; HRMS (M^+) calcd for $C_{72}H_{70}O_{11}S$ 1142.4639; found 1142.4648.

Compound 4. Compound **18** (0.466 g, 0.407 mmol), **10** (0.064 g, 0.204 mmol) and anhydrous K_2CO_3 (0.141 g, 1.02 mmol) in DMF (0.4 mL) were heated at 90 °C for 48 h under N_2 to give a crude solid that was purified by flash chromatography on silica gel (PhMe/EtOAc) to give **4** as yellow solid. Compound **4** could be further recrystallized from EtOAc−hexane to give analytically pure sample. (0.205 g, 0.090 mmol, 44%) mp 120−125 °C; $[\alpha]^{25.6}_D$ = +28.05 (*c* = 0.93, CH_2Cl_2). ^{1}H NMR (400 MHz, $CDCl_3$) δ 7.29−7.53 (m, 48 H), 6.85−7.11 (m, 42 H), 5.15 (s, 4 H), 4.53−4.52 (m, 8 H), 4.30−4.24 (m, 16 H), 1.535(s, 6 H), 1.528 (s, 6 H). 1.522 (s, 6 H), 1.513 (s, 6 H); ^{13}C NMR (100 MHz, $CDCl_3$) δ 156.2, 155.81, 155.78, 155.75, 137.2, 137.1, 136.91, 136.88, 129.15, 129.11, 128.97, 128.69, 128.62, 128.55, 127.93, 127.32, 126.95, 126.94, 126.83, 126.77, 126.74, 126.62, 126.55, 126.48, 123.26, 122.89, 122.81, 121.54, 121.16, 112.74, 112.39, 110.29, 110.27, 77.23, 76.91, 70.52, 69.06, 27.20; MS *m/z* FAB (NBA) 2257.4. Anal. Calcd for $C_{152}H_{142}O_{18}$: C, 80.90; H, 6.34; O, 12.76. Found: C, 80.59; H, 6.26.

Polymers 5 and 6. Compound **10** (0.343 g, 1.09 mmol), **13** (0.518 g, 1.10 mmol), and anhydrous K_2CO_3 (0.753 g, 5.45 mmol) in DMF (1 mL) were reacted at 90 °C for 48 h under N_2. DMF (0.5 mL) was refilled once for every 12 h in order to keep the mixture wet. 3,5-Dimethylphenol (0.027 g, 0.22 mmol) in DMF (0.3 mL) was added to end-cap the polymer. The mixture was further refluxed for 24 h and then diluted with $CHCl_3$ and filtered. The filtrate was concentrated to give a dark-

brown DMF solution. The polymer solution was precipitated by addition of the solution to MeOH to give yellowish solid that was further redissolved in $CHCl_3$ and reprecipitated from MeOH twice to give yellowish solid (0.253 g, 53%): $[\alpha]^{25.5}_D = +30.6$ ($c = 1.08$, CH_2Cl_2).^{1}H NMR (400 MHz, $CDCl_3$) δ 6.80−7.70 (ArH, 154 H), 4.20−4.60 (alkyl protons on the threitol moiety, 64 H), 2.20 (methyl group on the terminal unit, s, 6 H), 1.47−1.54 (methyl groups on the threitol unit, 64 H). The integration ratio of 10.7 between the methyl groups on the threitol units and the methyl groups on the terminal groups suggested that $n \sim 10-11$ for the polymer; ^{13}C NMR (100 MHz, $CDCl_3$) δ 155.74, 136.88, 129.10, 128.67, 126.88, 126.75, 126.52, 122,.86, 121.49, 112.34, 110.25, 77.20, 69.01, 27.17 Anal. Calcd. (for $n = 10$) $C_{314}H_{312}O_{44}$: C, 78.74; H, 6.57; O, 14.70. Found: C, 78.74; H, 6.57; O, 14.70.

Compound 7. General Procedure for 8 and 9. A stepwise synthetic sequence was adopted for preparation of compound **7**. In this procedure, **10** was first coupled with **14** to give the corresponding threitol monoether **22**, followed by methylation to give **7.** Following is the preparation procedure of the corresponding threitol monoether intermediate. Compound **14** (0.470 g, 1.48 mmol), **10** (0.661 g, 1.63 mmol), and anhydrous K_2CO_3 (0.616 g, 4.46 mmol) in DMSO (1 mL) were reacted at 90 °C for 10 h under N_2. The resulting mixture was finally quenched with 1N HCl. The product was extracted with ethyl acetate (3 × 30 mL). The organic extracts were collected, washed with saturated brine, dried over anhydrous $MgSO_4$, concentrated, and purified by flash chromatography on silica gel (EtOAc:PhMe = 1:5) to give the corresponding threitol monoether **22** as yellowish glassy solid (0.687 g, 1.23 mmol, 89%); $[\alpha]^{26.2}_D = +11.33$ ($c = 0.83$, CH_2Cl_2) ^{1}H NMR (400 MHz, $CDCl_3$) δ 7.61 (t, $J = 6.7$ Hz, 2 H), 7.55 (d, $J = 16.5$ Hz, 1 H), 7.50−7.45 (m, 7 H), 7.40 (t, $J = 7.1$ Hz, 2 H), 7.34 (t, $J = 7.2$ Hz, 1 H), 7.20 (t, $J = 8.3$ Hz, 2 H), 7.15 (d, $J = 16.4$ Hz, 1 H), 7.09 (d, $J = 16.4$ Hz, 1 H), 7.00 (t, $J = 6.8$ Hz, 1 H), 6.96 (t, $J = 6.8$ Hz, 1 H), 6.92 (d, $J = 8.2$ Hz, 1 H), 6.90 (d, $J = 8.3$ Hz, 1 H), 5.16 (s, 2 H), 4.39−4.35 (m, 1 H), 4.24−4.18 (m, 2 H), 4.16−4.12 (m, 1 H), 3.97−3.92 (m, 1 H), 3.81−3.75 (m, 1 H), 2.03−2.00 (m, 1 H), 1.50 (s, 6 H); ^{13}C NMR (100 MHz, $CDCl_3$) δ 156.1, 156.7, 137.2, 137.1, 136.9, 129.1, 128.9, 128.6, 127.9, 127.2, 126.9, 126.8, 126.6, 126.4, 123.3, 122.7, 121.5, 121.1, 112.7, 112.3, 109.7, 79.2, 75.3, 70.4, 68.6, 62.1, 27.12, 27.05; HRMS (M^+) calcd for $C_{36}H_{36}O_5$: 548.2563; found 548.2554. The threitol monoether **22** was further methylated to form **7** according to the following procedure. To a mixture of NaH (0.018 g of 60 wt % in mineral oil, 0.46 mmol) was prewashed with distilled hexane (3 × 3 mL) in THF (0.2 mL) at 0 °C was added the above threitol monoether (0.110 g, 0.20 mmol) under nitrogen. After reaction for 10 min, dimethylsulfate (0.058 g, 0.46 mmol) in THF (0.2 mL) was the added at 0 °C. The mixture is allowed to react at room temperature overnight and quenched by addition of water. The mixture was extracted with EtOAc (3 × 30 mL). The extracts were collected, washed with saturated brine, dried over anhydrous $MgSO_4$, concentrated, and purified by flash chromatography on silica gel (toluene) to give **7** as yellow solid (0.105 g, 0.18 mmol, 88%); mp 116−117 °C; $[\alpha]^{26.3}_D = +10.34$ ($c = 1.47$, CH_2Cl_2); ^{1}H NMR (400 MHz, $CDCl_3$) δ 7.61 (t, $J = 6.0$ Hz, 2 H), 7.54 (d, $J = 16.5$ Hz, 1 H), 7.51−7.46 (m, 7H), 7.41 (t, $J = 7.3$ Hz, 2H), 7.34 (t, $J = 7.2$ Hz, 1 H), 7.20 (t, $J = 7.3$ Hz, 2 H), 7.15 (d, $J = 16.4$ Hz, 1 H), 7.09 (d, $J = 16.3$ Hz, 1 H), 7.01−6.98 (m, 2 H), 6.95 (d, $J = 8.4$ Hz, 1 H), 6.90 (d, $J = 8.2$ Hz, 1 H), 5.15 (s, 2 H), 4.25−4.22 (m, 3 H), 4.15−4.13 (m, 1 H), 3.66−3.64 (m, 2 H), 3.38 (s, 3 H), 1.50 (s, 3 H), 1.49 (s, 3 H); ^{13}C NMR (100 MHz, $CDCl_3$) δ 156.1, 155.8, 137.2, 137.1, 137.0, 129.0, 128.9, 128.59, 128.57, 127.9, 127.2, 126.88, 126.87, 126.79, 126.6, 126.4, 123.3, 122.9, 121.4, 121.1, 112.7, 112.3, 110.0, 77.8, 76.5, 73.3, 70.5, 68.9, 59.5, 27.12, 27.00; HRMS (M^+) calcd for $C_{37}H_{38}O_5$: 562.2719; found 562.2725. Anal. Calcd for $C_{37}H_{38}O_5$: C, 78.98; H, 6.81; O, 14.22. Found: C, 78.98; H, 7.06.

Compound 8. 1,4-(*E,E*)-Bis(2′-hydroxy-4′-methylstyryl)benzene monobenzyl ether was first coupled with **14** to give the corresponding threitol monoether, followed by methylation to give **8.** Analytical data for the corresponding threitol monoether intermediate **23** (69.3% yield): mp 100−102 °C; ^{1}H NMR (400 MHz, $CDCl_3$) δ 7.50−7.33 (m, 13 H), 7.09 (d, $J = 16$ Hz, 1 H), 7.03 (d, $J = 16$ Hz, 1 H), 6.81−6.78 (m, 2 H), 6.77 (s, 1 H), 6.71 (s, 1 H), 5.13 (s, 2 H), 4.37−4.34 (m, 1 H), 4.24−4.17 (m, 2 H), 4.14−4.10 (m, 1 H), 3.94−3.93 (m, 1 H), 3.81−3.78 (m, 1 H), 2.34 (d, $J = 2.8$ Hz, 6 H), 1.92 (dd, $J = 5.2$ Hz, 7.6 Hz, 1 H), 1.50 (s, 6 H); ^{13}C NMR (100 MHz, $CDCl_3$) δ 155.89, 155.41, 138.71, 138.64, 137.10, 137.06, 136.74, 128.43, 128.03, 127.84, 127.71, 127.15, 126.58, 126.51, 126.32, 126.11, 124.01, 123.12, 122.50, 122.19, 121.82, 113.51, 113.16, 109.62, 79.32, 75.31, 70.49, 68.70, 62.18, 27.25, 27.19, 21.77, 21.72; HRMS (FAB) calcd for $C_{38}H_{40}O_5$ 576.2876; obsd 576.2877. Analytical data for **8** (75% yield): mp 98−100 °C; ^{1}H NMR (400 MHz, $CDCl_3$) δ 7.54−7.36 (m, 13 H), 7.13 (d, $J = 16$ Hz, 1H), 7.07 (d, $J = 16$ Hz, 1H), 6.82(d, $J = 8$ Hz, 2 H), 6.81 (s, 1H), 6.75 (s, 1 H), 5.14 (s, 2H), 4.27−4.23 (m, 3 H), 4.16−4.13 (m, 1 H), 3.71−3.66 (m, 2 H), 3.41 (s, 3 H), 2.37 (d, $J = 2.8$ Hz, 6 H), 1.53 (d, $J = 2.8$ Hz, 6 H); ^{13}C NMR (100 MHz, $CDCl_3$) δ 155.85, 155.43, 138.65, 138.61, 137.04, 137.00, 136.76, 128.38, 127.84, 127.77, 127.68, 127.11, 126.50, 126.29, 126.00, 123.91, 123.07, 122.62, 122.04, 121.79, 113.43, 113.03, 109.83, 77.84, 76.39, 73.34, 70.43, 68.92, 59.51, 27.21, 27.10, 21.74, 21.71; HRMS (FAB) calcd for $C_{39}H_{42}O_5$ 590.3032; obsd 590.3029.

Compound 9. 1,4-(*E,E*)-Bis(2′-hydroxy-4′-ethylstyryl)benzene monobenzyl ether was first coupled with **14** to give the corresponding threitol monoether, followed by methylation to give **9.** Analytical data for the corresponding threitol monoether intermediate **24** (63.1% yield): mp 120−122 °C; ^{1}H NMR (400 MHz, $CDCl_3$) δ 7.55−7.33 (m, 13 H), 7.12 (d, $J = 16$ Hz, 1H), 7.06 (d, $J = 16$ Hz, 1H), 6.84 (d, $J = 8$ Hz, 2 H), 6.81 (s, 1H), 6.76 (s, 1 H), 5.16 (s, 2 H), 4.40−4.36 (m, 1 H), 4.27−4.13 (m, 3 H), 3.99−3.94 (m, 1 H), 3.84−3.78 (m, 1 H), 2.69−2.62 (m, 4 H), 2.04 (s, 1 H), 1.52 (s, 6 H), 1.29−1.24 (m, 6 H); ^{13}C NMR (100 MHz, $CDCl_3$) δ 155.92, 155.47, 145.11, 145.03, 137.06, 137.03, 136.71, 128.38, 128.03, 127.85, 127.67, 127.16, 126.55, 126.49, 126.36, 126.15, 124.20, 124.17, 123.10, 122.49, 120.90, 120.52, 112.33, 111.93, 109.57, 79.27, 75.31, 70.47, 68.63, 62.14, 29.06, 27.21, 27.16, 15.61; HRMS (FAB) calcd for $C_{40}H_{44}O_5$ 604.3189; obsd 604.3193. Analytical data for **9** (70.3% yield): mp 84−85 °C; ^{1}H NMR (400 MHz, $CDCl_3$) δ 7.53−7.31 (m, 13 H), 7.10 (d, $J = 16$ Hz, 1 H), 7.04 (d, $J = 16$ Hz, 1H), 6.82 (d, $J = 8.0$ Hz, 2 H), 6.80 (s, 1H); 6.74 (s, 1 H), 5.14 (s, 2 H), 4.23 (d, $J = 6.0$ Hz, 3 H), 4.14−4.12 (m, 1 H), 3.66−3.65 (m, 2 H), 3.37(s, 3 H), 2.67−2.61 (m, 4 H), 1.49 (d, $J = 2.8$ Hz, 6 H), 1.26−1.21 (m, 6 H); ^{13}C NMR (100 MHz, $CDCl_3$) δ 155.98, 155.57, 145.18, 145.11, 137.11, 137.06, 136.82, 128.42, 127.97, 127.89, 127.73, 127.21, 126.54, 126.41, 126.13, 124.24, 124.21, 123.15, 122.70, 120.84, 120.57, 112.39, 111.94, 109.88, 77.93, 76.45, 73.38, 70.55, 69.00, 59.56, 29.11, 27.25, 27.14, 15.62; HRMS (FAB) calcd for $C_{41}H_{46}O_5$ 618.3345; obsd 618.3340.

Acknowledgment. We thank the National Science Council of Taiwan (NSC 95-2113-M002-021-MY3, NSC 98-2119-

M002-006-MY3, and NSC 97-3114-M002-005), Academia Sinica (Thematic Project), Ministry of Education of Taiwan, and National Taiwan University for financial support.

Supporting Information Available: ^{1}H NMR spectra of **1**−**5**, **7**−**12**, **15**−**16**, **19**−**24**. This material is available free of charge via the Internet at http://pubs.acs.org.

References and Notes

(1) (a) Fan, J.; Boettcher, S. W.; Tsung, C.-K.; Shi, Q.; Schierhorn, M.; Stucky, G. D. *Chem. Mater.* **2008**, *20*, 909–921. (b) Pijper, D.; Feringa, B. L. *Soft Matter* **2008**, *4*, 1349. (c) Pieraccini, S.; Ferrarini, A.; Spada, G. P. *Chirality* **2008**, *20*, 749. (d) Feringa, B. L.; van Delden, R. A.; ter Wiel, M. K. J. *Pure Appl. Chem.* **2003**, *75*, 563. (e) Dumus, D.; Goodby, J.; Gray, G. W.; Spiess, H.-W. *Handbook of Liquid Crystals*; Wiley-VCH: New York, 1998. (f) Crawford, G. P. *IEEE Spectrum* **2000**, *37*, 10–40. (g) Yang, D.-K.; Wu, S.-T. *Fundamentals of Liquid Crystal Devices*; John Wiley & Sons: New York, 2006. (h) Witte, P.; Brehmer, M.; Lub, J. *J. Mater. Chem.* **1999**, *9*, 2087. (i) Yamaguchi, T.; Inagawa, T.; Nakazumi, H.; Irie, S.; Irie, M. *Chem. Mater.* **2000**, *12*, 869. (j) Funahashi, M.; Tamaoki, N. *Chem. Mater.* **2007**, *19*, 608. (k) Kurihara, S.; Nomiyama, S.; Nonaka, T. *Chem. Mater.* **2001**, *13*, 1992. (l) Sung, C.-H.; Kung, L.-R.; Hsu, C.-S.; Lin, T.-F.; Ho, R.-M. *Chem. Mater.* **2006**, *18*, 352. (m) Lin, T.-F.; Ho, R.-M.; Sung, C.-H.; Hsu, C.-S. *Chem. Mater.* **2008**, *20*, 1404. (n) Mitsuoka, T.; Sato, H.; Yoshida, J.; Yamagishi, A.; Einaga, Y. *Chem. Mater.* **2006**, *18*, 3442. (o) Ouahab, L. *Chem. Mater.* **1997**, *9*, 1909. (p) Pecinovsky, C. S.; Nicodemus, G. D.; Gin, D. L. *Chem. Mater.* **2005**, *17*, 4889.

(2) (a) Reinitzer, F. *Monatsh. Chem.* **1888**, *9*, 421. (b) Ferrarini, A.; Moro, G. J.; Nordio, P. L. *Mol. Phys.* **1996**, *87*, 485. (c) Pieraccini, S.; Ferrarini, A.; Gottarelli, G.; Lena, S.; Masiero, S.; Spada, G. P. *J. Org. Chem.* **2005**, *70*, 8009. (d) Wilson, M. R.; Earl, D. J. *J. Chem. Phys.* **2003**, *119*, 10280. (e) Neal, M. P.; Solymosi, M. *J. Chem. Phys.* **2003**, *119*, 3567. (f) Cook, M. J.; Wilson, M. R. *J. Chem. Phys.* **2000**, *112*, 1560. (g) Vizitiu, D.; Lazar, C.; Radke, J. P.; Hartley, C. S.; Glaser, M. A.; Lemieux, R. P. *Chem. Mater.* **2001**, *13*, 1692. (h) Hartley, C. S.; Wang, R.; Lemieux, R. P. *Chem. Mater.* **2004**, *16*, 5297. (i) van Dijk, L.; Kersten, S. P.; Jonkheijm, P.; van der Schoot, P.; Bobbert, P. A. *J. Phys. Chem. B* **2008**, *112*, 12386. (j) Sumpter, B. G.; Kumar, P.; Mehta, A.; Barnes, M. D.; Shelton, W. A.; Harrison, R. J *J. Phys. Chem. B* **2005**, *109*, 7671. (k) Nakayama, H.; Kimura, S. *J. Org. Chem.* **2009**, *74*, 3462.

(3) Reviews of chiral dopants: (a) Gottarelli, G. ; Solladié, G.; Spada, G. P. *Nouv. J. Chim.* **1986**, *10*, 691. (b) Solladié, G.; Zimmermann, R. G. *Angew. Chem., Int. Ed.* **1984**, *23*, 348. (b) Spada, G. P.; Proni, G. *Enantiomer* **1998**, *3*, 301. (c) Proni, G.; Spada, G. P. *Enantiomer* **2001**, *6*, 171. (d) Gottarelli, G.; Spada, G. P. *Top. Stereochem.* **2003**, *24*, 425. (e) Feringa, B. L.; Eelkema, R. *Org. Biomol. Chem.* **2006**, *4*, 3729.

(4) (a) Maeda, K.; Takeyama, Y.; Sakajiri, K.; Yashima, E. *J. Am. Chem. Soc.* **2004**, *126*, 12684. (b) Eelkema, R.; Feringa, B. L. *J. Am. Chem. Soc.* **2005**, *127*, 13480. (c) Eelkema, R.; Feringa, B. L. *Org. Lett.* **2006**, *8*, 1331. (b) Ikemoto, T.; Mitsuhashi, K.; Mori, K. *Tetrahedron: Asymmetry* **1993**, *4*, 687. (a) Feringa, B. L.; van Delden, R. A. *Angew. Chem.* **2001**, *40*, 3198. (b) Feringa, B. L.; van Delden, R. A. *Chem. Commun.* **2002**, 174.

(5) Kitzerow, H.-S.; Bahr, C. *Chirality in Liquid Crystals*; Springer: New York, 2001.

(6) Rinaldi, P. L.; Naidu, M. S. R.; Conaway, W. E. *J. Org. Chem.* **1982**, *47*, 3987.

(7) (a) Kuball, H.-G.; Weiss, B.; Beck, A. K.; Seebach, D. *Helv. Chim. Acta* **1997**, *80*, 2507. (b) Seed, A. J.; Walsh, M. E. *Mol. Cryst. Liq. Cryst.* **2004**, *410*, 201. (c) Seebach, D.; Beck, A. K.; Heckle, A. *Angew. Chem., Int. Ed.* **2001**, *40*, 92.

(8) (a) Rosini, C.; Spada, G. P.; Proni, G.; Masiero, S.; Scamuzzi, S. *J. Am. Chem. Soc.* **1997**, *119*, 506. (b) Superchi, S.; Donnoli, M. I.; Proni, G.; Spada, G. P.; Rosini, C. *J. Org. Chem.* **1999**, *64*, 4762. (c) Pieraccini, S.; Ferrarini, A.; Gottarelli, G.; Lena, S.; Masiero, S.; Spada, G. P. *J. Org. Chem.* **2005**, *70*, 8009.

(9) (a) Gottarelli, G.; Hibert, M.; Samori, B.; Spada, G. P.; Zimmermann, R. *J. Am. Chem. Soc.* **1983**, *105*, 7318. (b) Gottarelli, G.; Spada, G. P. *J. Org. Chem.* **1986**, *51*, 589. (c) Rosini, C.; Rosati, I.; Spada, G. P. *Chirality* **1995**, *7*, 353. (d) Proni, G.; Spada, G. P.; Lustenburger, P.; Welti, R.; Diederich, J. *J. Org. Chem.* **2000**, *65*, 5522. (e) Bandin, M.; Casolari, S.; Cozzi, P. G.; Proni, G.; Schmohel, E.; Spada, G. P.; Tagliavini, E.; Umani-Ronchi, A. *Eur. J. Org. Chem.* **2000**, *491*. (f) Goh, M.; Matsushita, T.; Kyotani, M.; Akagi, K. *Macromolecules* **2007**, *40*, 4762.

(10) (a) Gottarelli, G.; Osipov, M. A.; Spada, G. P. *J. Phys. Chem.* **1991**, *95*, 3879. (b) Matteo, A. D.; Todd, S. M.; Gottarelli, G.; Solladié, G.; Williams, V. E.; Lemieux, R. P.; Ferrarini, A.; Spada, G. P. *J. Am. Chem. Soc.* **2001**, *123*, 7842. (c) Holzwarth, R.; Bartsch, R.; Cherkaoui, Z.; Solladié, G. *Chem.*−*Eur. J.* **2004**, *10*, 3931.

(11) (a) Ferrarini, A.; Gottarelli, G.; Nordio, P. L; Spada, G. P. *J. Chem. Soc., Perkin Trans.* **1999**, *2*, 411. (b) Feringa, B. L.; van Delden, R. A.; Koumura, N.; Geertsema, E. M. *Chem. Rev.* **2000**, *100*, 1789. (c) Chou, Y.-C.; Chen, C.-T. *J. Am. Chem. Soc.* **2000**, *122*, 7662.

(12) (a) Yoshida, J.; Sato, H.; Yamagishi, A.; Hoshino, N. *J. Am. Chem. Soc.* **2005**, *127*, 8453. (b) Hoshino, N.; Matsuoka, Y.; Okamoto, K.; Yamagishi, A. *J. Am. Chem. Soc.* **2003**, *125*, 1718.

(13) Ruxer, J. M.; Solladié, B.; Candau, S. *Mol. Cryst. Liq. Cryst.* **1978**, *41*, 109.

(14) (a) Pieraccini, S.; Ferrarini, A.; Fuji, K.; Gottarelli, G.; Lena, S.; Tsubaki, K.; Spada, G. P. *Chem.*−*Eur. J.* **2006**, *12*, 1121. (b) Kuball, H.-G.; Brüning, H. *Chirality* **1997**, *9*, 407.

(15) Yang, C. F.; Chen, H.-D.; Yang, K. H.; Leung, M.-k.; Wu, C.-C.; Yang, C. C.; Wang, C. C.; Fann, W. S *Mater. Sci. Eng.* **2001**, *85* (2−3), 236.

(16) Chow, H. F.; Mak, C. H. *J. Chem. Soc., Perkin Trans. 1* **1997**, 91.

(17) (a) Palik, M.; Karlubikova, O.; Lasikova, A.; Kozisek, J.; Gracza, T. *Eur. J. Org. Chem.* **2009**, *5*, 709. (b) Wroblewski, A. E.; Glowacka, I. E. *Tetrahedron* **2005**, *61*, 11930. (c) Fujimoto, Y.; Satoh, M.; Takeuchi, N.; Kirisawa, M. *Chem. Pharm. Bull.* **1990**, *38*, 1447. (d) Bouzide, A.; Sauve, G. *Org. Lett.* **2002**, *4*, 2329.

(18) Instead of using *R*-(-) and *S*-(+)-2,2′-binaphthyl-1,1′-diol as the standard, cholesteryl oleyl carbonate has been used as a standard chiral nematic LC. More detailed methods are depicted in: (a) Goh, M,; Kyotani, M.; Akagi, K *J. Am. Chem. Soc.* **2007**, *129*, 8519–8527. (b) Goh, M.; Akagi, K. *Liq. Cryst.* **2008**, *35*, 953–965.

(19) (a) Kimura, H.; Hosino, M.; Nakano, H. *J. Phys. Colloq.* **1979**, *40* (C3), 174. (b) Kutulya, L.; Vashchenko, V.; Semenkova, G.; Shkolnikova, N. *Mol. Cryst. Liq. Cryst.* **1999**, *331*, 2443–2451. (c) Kutulya, L.; Vashchenko, V.; Semenkova, G.; Shkolnikova, N.; Drushlyak, T.; Goodby, J. *Mol. Cryst. Liq. Cryst.* **2001**, *361*, 125–134. (d) Akagi, K.; Higuchi, I.; Piao, G.; Shirakawa, H.; Kyotani, M. *Mol. Cryst. Liq. Cryst.* **1999**, *332*, 463. (e) Piao, G.; Akagi, K.; Shirakawa, H.; Kyotani, M. *Curr. Appl. Phys.* **2001**, *1*, 121. (f) Tang, K.; Green, M. M.; Cheon, K. S.; Selinger, J. V.; Garetz, B. A. *J. Am. Chem. Soc.* **2003**, *125*, 7313–7323.

(20) (a) Tamaki, R.; Samura, K.; Chujo, Y. *J. Chem. Soc., Chem. Commun.* **1998**, 1131. (b) Gottarelli, G.; Spada, G. P. *Mol. Cryst. Liq. Cryst.* **1985**, *123*, 377.

(21) A polyimide-coated antiparallel rubbed, 5 μm, ITO cell. Commercially available from Mesostate LCD Industries, Co., Ltd., Taiwan; used as received.

(22) For AM1 method, see: (a) Dewar, M. J. S.; Zoebisch, E. G.; Healy, E. F; Stewart, J. J. P. *J. Am. Chem. Soc.* **1985**, *107*, 3902–3909. For ZINDO method, see: (b) Bacon, A. D.; Zerner, M. C. *Theor. Chim. Acta* **1979**, *53*, 21. (b) Correa de Mello, P.; Hehenberger, M.; Zerner, M. C *Int. J. Quantum Chem.* **1982**, *21*, 251. (c) Zerner, M. C. *J. Chem. Phys.* **1975**, *62*, 2788. (d) Zerner, M. C. *Reviews in Computational Chemistry*; Limpkowitz, K. B., Boyd, D. B., Eds.; VCH Publishing: New York, 1991; Vol. 2, pp 313−366.

(23) (a) Gottarelli, G.; Samori, B.; Marzochi, S.; Stremmenos, C. *Tetrahedron Lett.* **1975**, *24*, 1981. (b) Kinaldi, P. L.; Wilk, M. *J. Org. Chem.* **1983**, *48*, 2141.

(24) (a) The calculations were performed using the software of CAChe, Fujisu. (b) For PM3 method, see: Stewart, J. J. P. *J. Comput. Chem.* **1989**, *10*, 209–220. (c) For PM5 method, see: Stewart, J. J. P. *J. Comput. Chem.* **1991**, *12*, 320.

JP909286T